HOLOS
ISSN 1807 - 1600

ANÁLISE NUMÉRICA TRANSIENTE TÉRMICA ESTRUTURAL DE TENSÕES RESIDUAIS EM VASOS DE PRESSÃO CILÍNDRICOS SUBMETIDOS A REPARO DE SOLDAGEM DE ACORDO COM A NORMA ASME PCC-2-2015

J. I. L. ALMEIDA[1], M. C. RODRIGUES[2], P. F. CAVALCANTE[3]
Universidade Federal da Bahia[1,3], Universidade Federal da Paraíba[2]
ORCID ID: https://orcid.org/0000-0001-6899-920X[1]
jayann.ismar@gmail.com[1]

RESUMO

Este artigo apresenta o cálculo de tensões residuais presentes em vasos de pressão cilíndricos submetidos a reparos de solda usando o padrão ASME PCC-2-2015 via análise numérica multifísica transiente térmica estrutural utilizando o método dos elementos finitos. Os métodos de análise de tensão residual por análise numérica vêm cada vez mais fazendo parte da dinâmica de integridade estrutural em equipamentos como vasos de pressão, flanges, trocadores de calor, além de observar o comportamento dessas tensões nas áreas afetadas termicamente devido a processos de soldagem. No reparo de soldagem, a luva é presa ao vaso de pressão através de duas soldas longitudinais e duas soldas transversais. A modelagem do vaso de pressão, reparo e soldagem foram realizadas de acordo com a norma citada. Os parâmetros de soldagem foram adotados com o que acontece na prática, e com isso foram obtidas a distribuição de temperatura e fluxo de calor. Os objetivos foram analisar as tensões longitudinais, tangenciais e residuais nas regiões da solda, vaso de pressão e reparo durante o período de soldagem, e verificar o comportamento dessas tensões após o período de resfriamento. Este trabalho mostra que a análise numérica pode ser usada com eficiência e objetividade em situações de controle e conhecimento da integridade estrutural de equipamentos.

PALAVRAS-CHAVE: Tensões Residuais, Vasos de Pressão, Reparos, Elementos Finitos.

STRUCTURAL THERMAL TRANSIENT NUMERICAL ANALYSIS OF RESIDUAL STRESSES IN CYLINDRICAL PRESSURE VESSELS SUBMITTED TO WELD REPAIR ACCORDING TO STANDARD ASME PCC-2-2015

ABSTRACT

This paper presents the calculation of residual stresses present in cylindrical pressure vessels subjected to weld repairs using the ASME PCC-2-2015 via numerical multiphysical thermal structural analysis using the finite element method. The methods of analysis of residual stress by numerical analysis are increasingly part of the dynamics of structural integrity in equipment such as pressure vessels, flanges, heat exchangers, in addition to observing the behavior of these stresses in the thermally affected areas due to welding processes. In welding repair, the sleeve is attached to the pressure vessel through two longitudinal welds and two transverse welds. The modeling of the pressure vessel, repair and welding were carried out according to the aforementioned standard. The welding parameters were adopted with what happens in practice, and with that the temperature distribution and heat flow were obtained. The objectives were to analyze the longitudinal, tangential and residual stresses in the regions of the weld, pressure vessel and repair during the welding period, and to verify the behavior of these stresses after the cooling period. This work shows that numerical analysis can be used efficiently and objectively in situations of control and knowledge of the structural integrity of equipment.

KEYWORDS: Residual Stresses, Pressure Vessels, Repairs, Finite Elements.

1 INTRODUCTION

In a simple way, residual stresses are understood as stresses that remain acting on the material even when all external forces are withdrawn. These stresses have elastic behavior, and may be beneficial to structures and equipment, depending on their magnitude, signal and distribution (LU, 2005).

The residual stresses are divided into three categories: macroscopic, microscopic and submicroscopic. The first tension mentioned, also called residual stress of type I, is homogeneous in the volume of several grains and causes almost uniform deformations in many grains according to HIRSCH (2006). They can be found in materials that have undergone non-uniform plastic deformation, such as folding, rolling process, thermal gradients and tempering of steels.

The study of residual stresses and corrosion in computational mechanics is very recent, since the advent of finite element techniques began only in the middle of the last century. But these studies are rapidly improving, and much work is being done.

For BAN (2013), residual stresses in welded sections of steels are mainly formed during welding and the consequent cooling process is associated with non-uniform plastic deformations. As one of the most important initial imperfections in welded steel profiles, this has significant effects on the load capacity, especially the buckling force of structural steel elements, resulting in premature flow and loss of stiffness

In addition to the determination of residual stresses by various experimental techniques, a large amount of work has been carried out over many years in the finite element area for the determination of residual stresses in welds, Rybicki (1979). With the advent of several numerical models, MARTINEZ (1997) suggests that it is interesting to estimate by measurement or simulation in finite elements, the distribution of residual stresses in welded structures subjected to loads of external services.

In the oil and gas sector, an application that can be given to this type of equipment is in the performance of pipe repairs using the Type A or Type B dual channel method with interference. To ensure the condition of radial interference between the chutes and the duct, a clamping force is applied in the tangential direction to the pipe, the load being applied through concentric chains to the assembly on the chutes. Studies developed by Borges, Braga (5), show that the clamping force is one of the main parameters that guarantee the efficiency of this type of repair, and must be applied with accuracy and reliability.

2 METHODOLOGY

2.1 Methodology Modeling of the Pressure Vessel with Corrosion

The pressure vessel with corrosion can be modeled in SolidWorks 2014 software, as follows the step-by-step described below by Almeida (2012). The thickness loss profile of the region is obtained where each point is a longitudinal (horizontal) and circumferential (vertical) distance of

50.8 mm (2.0 in). Table (1) shows the values for the wall thickness of the vessel in the longitudinal and circumferential planes.

Table 1 - Values of the wall thickness of the pressure vessel for the longitudinal and circumferential planes.

plan (mm)	C1	C2	C3	C4	C5	C6	C7	C8
M1	19.05	19.05	19.05	19.05	19.05	19.05	19.05	19.05
M2	19.05	12.19	13.21	14.48	14.22	14.73	15.24	19.05
M3	19.05	14.48	14.99	13.97	14.99	15.24	16.76	19.05
M4	19.05	15.49	11.94	14.73	9.14	14.73	16.26	19.05
M5	19.05	15.75	14.99	14.73	14.48	12.19	15.75	19.05
M6	19.05	14.48	14.99	15.49	14.48	14.22	12.45	19.05
M7	19.05	19.05	19.05	19.05	19.05	19.05	19.05	19.05

From the origin of the Cartesian coordinate system, the rectangle is drawn, (the coordinates (x, y) are chosen by choice), the starting point is determined from the origin of the axis, distance from 609.6 mm (24 in), this measure is the inner radius of the pressure vessel. Through this point, the initial rectangular profile of the duct is modeled. The rectangular profile has a height corresponding to the nominal thickness of the pressure vessel of 19.05 mm (0.75 in) and the base corresponds to the width of the vessel to be modeled. The width should be greater than the sum of the longitudinal steps of the 355,60 mm (14 in) inspection points given by Tab. (1). Figure (1) shows the result of the rectangular profile where the base considered was 508 mm (20 in).
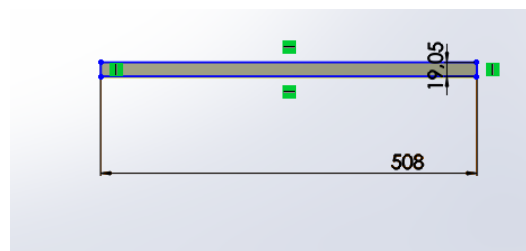
Figure 1 - Rectangular profile.

For vessel generation, the rectangular profile is used to initiate a surface generated in steps of arcs around its central axis. The angle for each arc is defined by Equation (1).

$$\alpha = L/r \tag{1}$$

Where α is the angle in radians of the arc, L is the step of each inspection and r is the nominal internal radius of the pressure vessel. Figure (2) shows the relation for calculating the angle of each arc in radians.
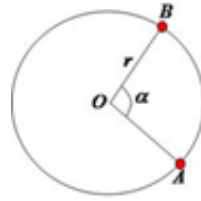
Figure 2 - Trigonometric relation for the central angle.

For this case the nominal internal radius of 609.6 mm (24 in) and the pitch between the collected points L of 38.1 mm (1.5 in), thus:

$$\alpha = L/r = 1.5/24 = 0.0625 \text{ rad} = 3.581° \cong 3.6°$$

With the angle of the calculated arc the volume formation is performed from the rectangular profile corresponding to a region unaffected by the damage, as shown in Figure (3).
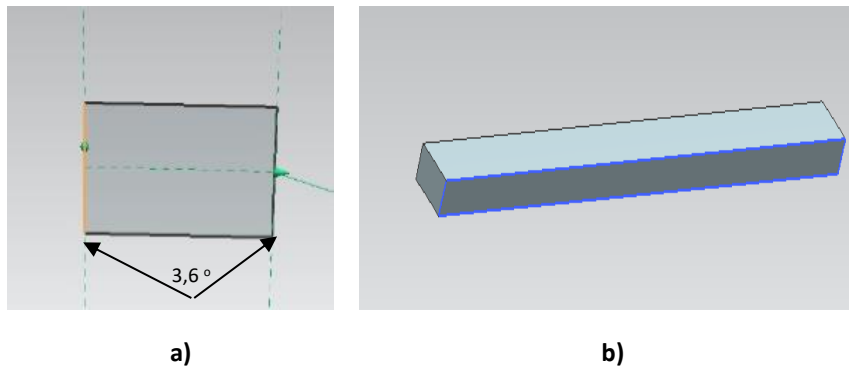

a)   b)

Figure 3 - (a) lateral view with the pitch of the arc and (b) first volume created.

Note that the angle is 3.6 °, as calculated, it is important to note also that each generated volume width corresponds to 508 mm (20 in), which is exactly the distance between each inspection point. Following the construction of all profiles according to Table (1), one can model the whole area of the corroded region through the steps explained above. After the modeling of the thicknesses, a complete view of the damage can be seen in Figure (4):

Figure 4 - Pressure vessel modeled with external corrosion.

2.2 Repair Modeling

The first step in modeling the repair is to check the width of the tool, since according to the standard the glove width must be 50.8 mm (2 in) apart from the corrosion damage. The defect width is 266.7 mm (10.5 in), as can be seen in Figure (5).
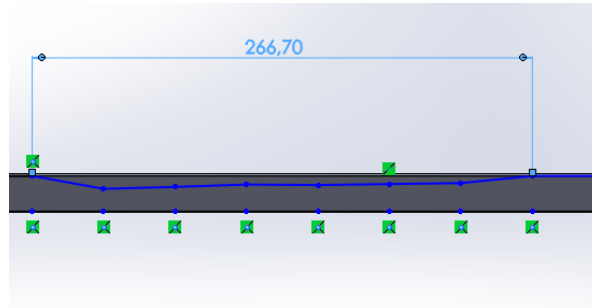

Figure 5 - Width of defect caused by corrosion.

Thus, the width of the repair should be at least 368.3 mm (14.5 in), to satisfy the criterion of the standard. As can be seen in Figure (6), the glove was modeled with the minimum allowable width.
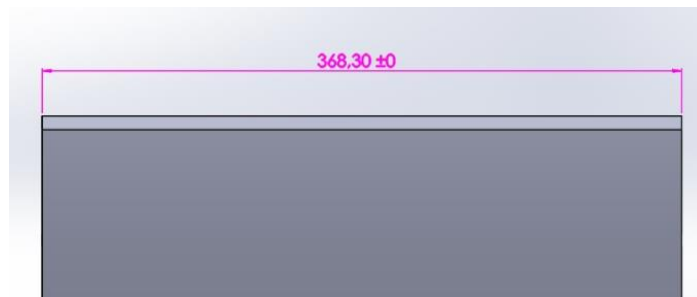

Figure 6 - Repair width modeling.

The internal diameter of the vessel is measured at the outer diameter of the vessel, the vessel inner diameter is known to be 1219.2 mm (48 in), and the thickness is 19.05 mm (0.75 in), With this according to Equation (2), the inner diameter of the glove is:

$$Dil = Div + 2e \tag{2}$$

On what:

Dil – Sleeve inner diameter;

Div – Vessel inner diameter;

e – Thickness of the vessel.

Thereby:

$$Dil = 12192+(2x19.05) => Dil = 1257.30 \text{ mm}$$

In other words, the internal radius of the glove is 628.65 mm (24.75 in), the thickness of the repair is 19.05 mm (0.75 in), therefore the external radius of the glove is 647, 70 mm (25.5 in), as shown in Figure (7).
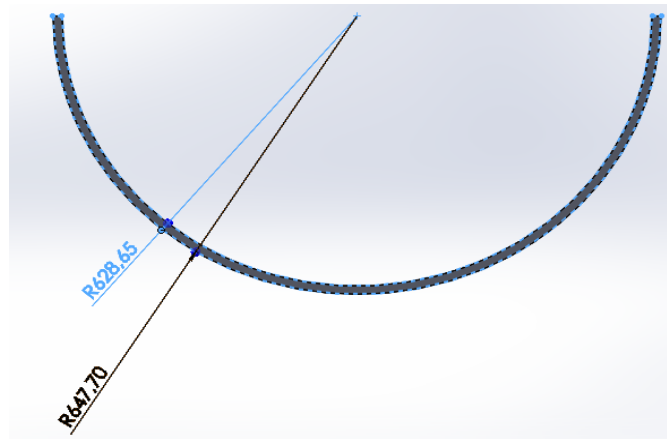

Figure 7 - Internal and external radius of the glove.

To finalize the modeling, two V-grooves were made in the diagonally opposite places on the glove for the realization of the weld, as can be seen in Figure (8).
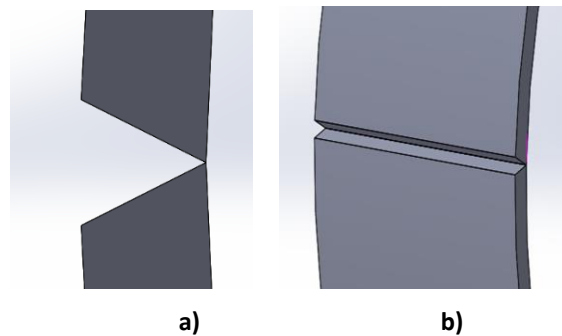

a)   b)

Figure 8 - Bevel Modeling of (a) V-Profile and (b) Throughout the width of the repair.

The angle of the V-groove is 45°, since this angle is often used in situations where the thickness of the parts is small, as is the case with the glove.

2.3 Welding Modeling

Finally, the weld beads are modeled: two longitudinal strands and two circumferential strands. The longitudinal weld has the same repair width and its complete modeling is shown in Figure (9).
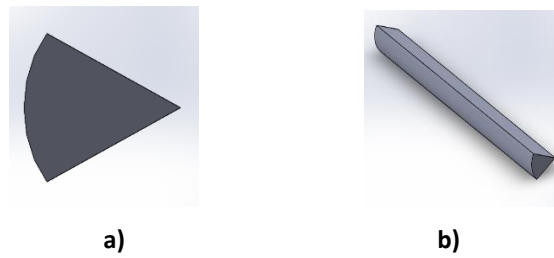
Figure 9 - Detail of the longitudinal weld (a) In profile and (b) In perspective.

For the modeling of the circumferential weld, it was made of an angular shape so that the cross section is triangular. Figure (10) shows the modeling of the circumferential weld.
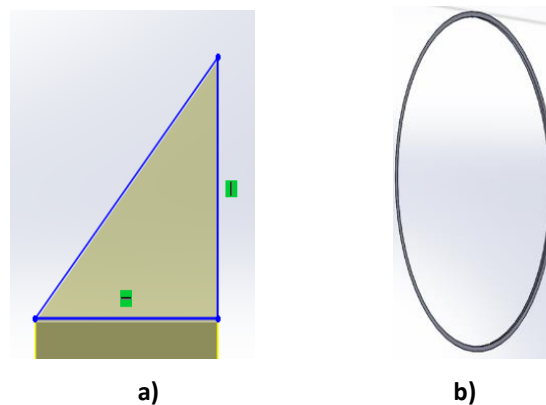

Figure 10 - Detail of the circumferential weld (a) In profile and (b) In perspective.

Finally, the complete modeling of the assembly can be seen in Figure (11).


Figure 11 - Complete modeling of the pressure vessel-repair-weld assembly.

As can be seen, only one circumferential and one longitudinal weld is observed, but the other two are at the back of the drawing.

3 RESULTS AND DISCUSSIONS

3.1 Analysis of the Longitudinal Residual Stresses Behavior in the First Longitudinal Weld Region

We selected 10 points to the left of the weld bead and 10 to the right spaced 20 mm to observe the behavior of the longitudinal stress in the thermally affected zone. This total distance of 200 mm covers the area where the stresses begin to be stable. Figure (12) shows the longitudinal stress distributions in the region of the thermally affected zone in this critical central region.
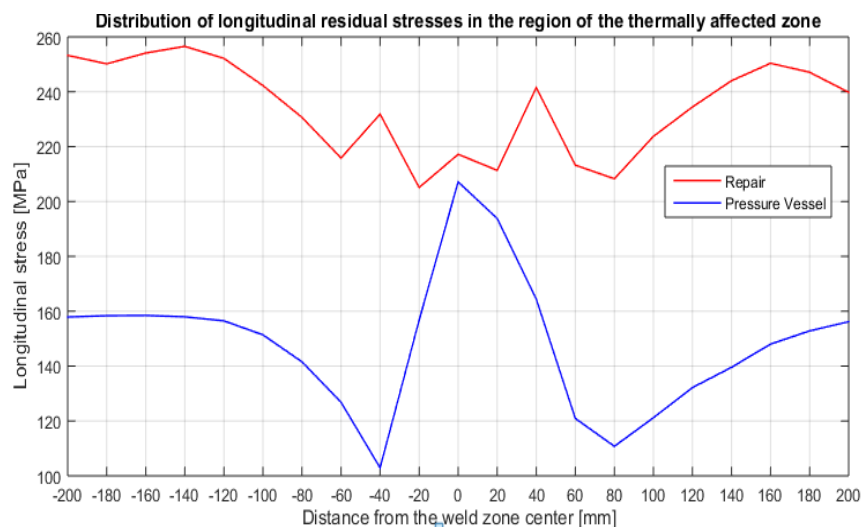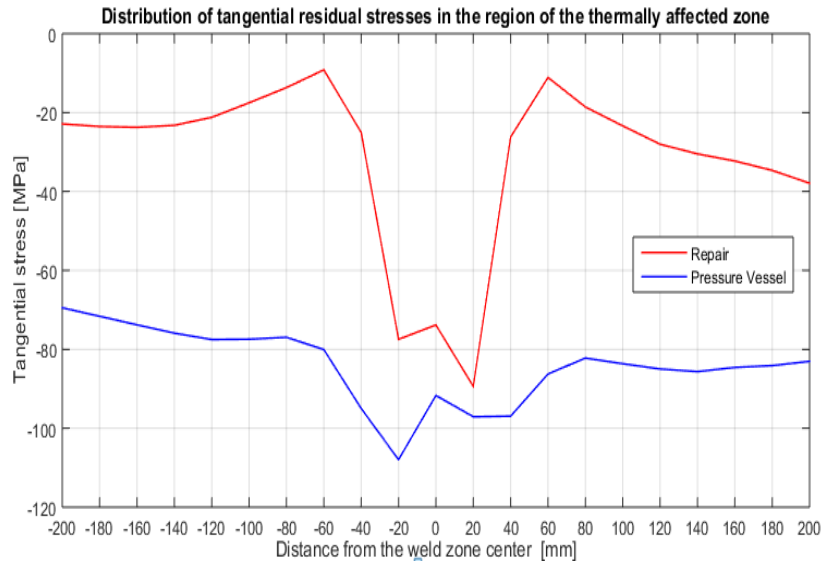

Figure 12 - Behavior of longitudinal stresses in the pressure vessel and repair in the first longitudinal weld.

It is observed that in Figure (12), the greatest longitudinal tensions are concentrated in the region of the weld, and for the repair, after a certain distance, the tensions are also high, which is not observed in the pressure vessel, which occurs A relief of these stress. At the center of the weld a stress of about 220 MPa is observed.

In the pressure vessel, as it moves away from the weld bead, these tensions decrease, becoming stable, close to 160 MPa, opposite situation was observed in the repair, where the tensions increase the mean that moves away from the weld bead. It can be seen in Figure 12 that the longitudinal stresses in the repair are all traction and oscillate greatly as it moves away from the center of the weld bead, having two peaks of tension in the region when removed about 40 mm, The stresses decrease in the range of 60 mm the tensions increase again, being soft after the 150 mm.

Similarly, the behavior of tangential stresses with respect to the center of the weld is observed, as can be seen in Figure (13).

Figure 13 - Behavior of the tangential stresses in the pressure vessel and repair in the first longitudinal weld.

The tangential stresses in the repair follow and in the pressure vessel are all of compression, as seen in Figure (13). In the repair, the stresses are smaller (in modulus), in relation to the stresses in the vessel. In the region between 20 and 60 mm, there is an increase in these stresses, followed by relief and stabilization.

In the pressure vessel, the compression stresses are higher, and the voltage peaks in the region between 20 and 60 mm are not observed, the behavior of these stresses is much smoother, stabilizing between -70 and -85 MPa. Finally, the behavior of the von Mises residual stresses in the pressure vessel and in the repair is analyzed in Figure (14).
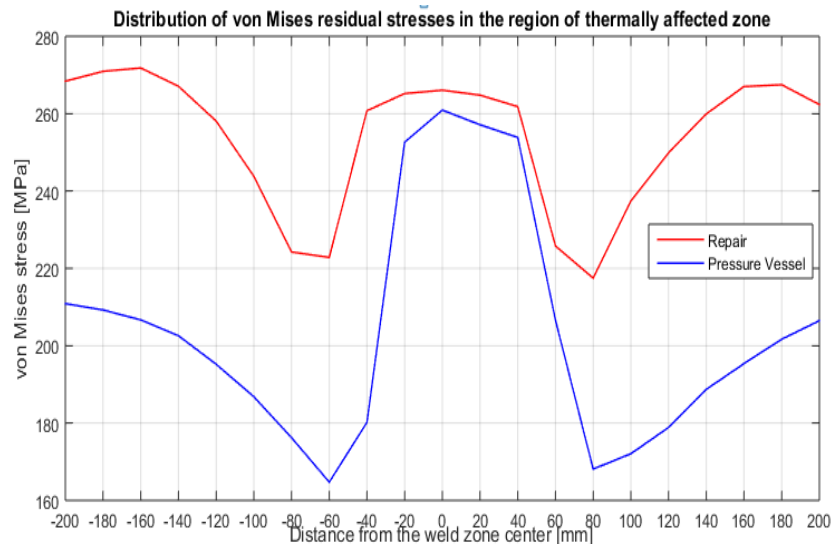
Figure 14 - Behavior of the von Mises stresses in the pressure vessel and repair in the first longitudinal weld.

It is observed in Figure (14) that the higher von Mises stresses in the repair are observed in the center of the weld and in the regions farthest from the same, having a decrease in the region between 50 and 75 mm until they are stable after the 150 mm from distance. Finally, the von Mises

tensions are maximal at the center of the weld in the pressure vessel, as can be seen in Fig. (14), with a value close to 260 MPa. Similarly in the repair, in which the von Mises stress decreases and after a certain distance from the center of the solder increases again, in the vessel follows the same pattern, but the observed stresses are smaller, with a stabilization around 210 MPa.

3.2 Analysis of the Behavior of Longitudinal Residual Stresses in the Second Longitudinal Weld Region

Similarly, 20 points symmetrically spaced 20 mm from the center of the second longitudinal weld were selected in the central region of the weld (critical) to observe the behavior of these voltages in relation to the thermally affected zone. The Figure (15) shows the behavior of longitudinal residual stresses in the repair and in the pressure vessel in the second longitudinal weld.
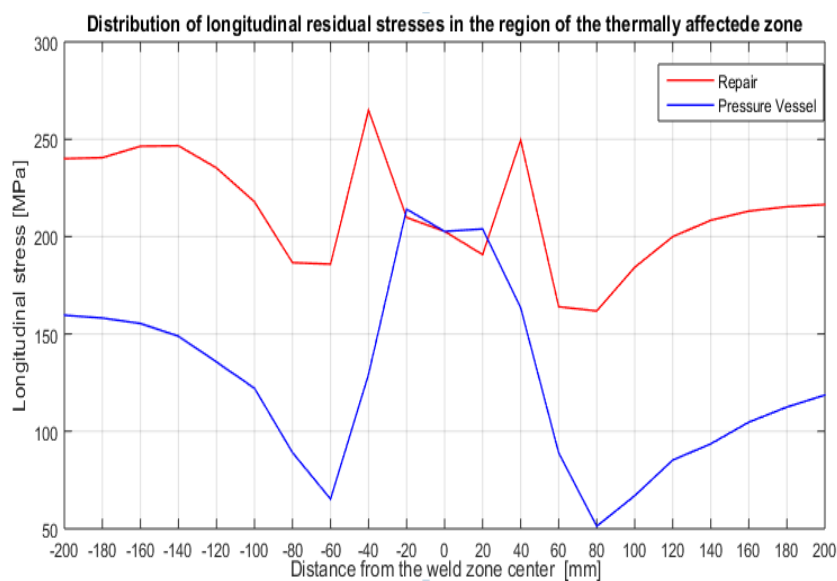

Figure 15 - Behavior of longitudinal stresses in the pressure vessel and repair in the second longitudinal weld.

There is a longitudinal stress in the center of the weld of about 200 MPa and two symmetrical stress peaks in the region about 40 mm away from the center of the weld during repair, after these peaks, there is a decrease in stress up to about 75 mm, and after that distance the stresses increase until they stabilize between 220 MPa and 240 MPa. In the pressure vessel, the greatest longitudinal stress occurs at the center of the weld, with a reduction of these stresses down to about 75 mm. After that, the stresses increase and stabilize between 120 and 160 MPa.

In Figure (16) it is seen that the tangential stress at the center of the weld is -90 MPa and in the repair these tensions increase up to about 40 mm, reaching tensile stresses of 10 MPa and as it moves away from the center of the weld, stabilizing between -40 MPa and -15 MPa.
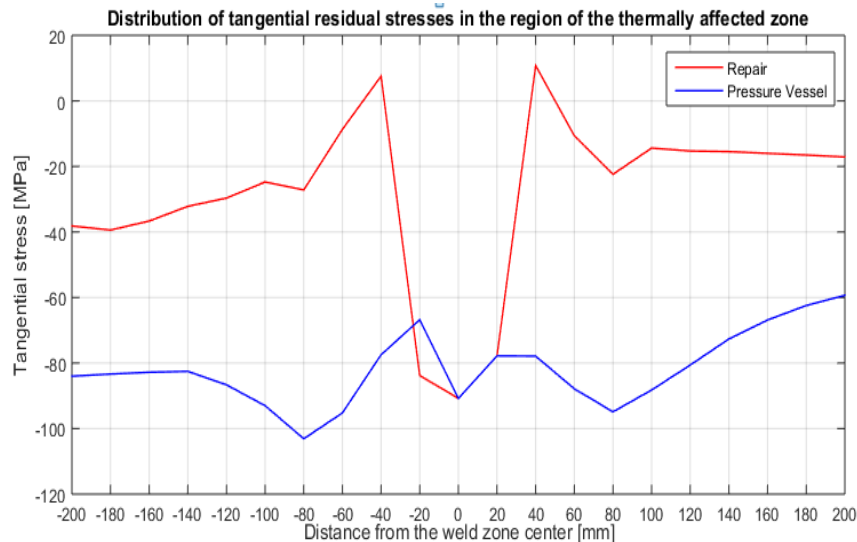
Figure 16 - Behavior of the tangential stresses in the pressure vessel and repair in the second longitudinal weld.

At tangential stresses, a compression stress of -90 MPa, which is found in the repair, is also present in the center of the weld, and these compressive stresses decrease up to about 25 mm, increase back to about 75 mm, and after at a distance of 200 mm, the stresses are between -85 and -60 MPa. In order to finish the analysis in the second weld, the behavior of the residual stresses of von Mises in relation to the center of the weld is observed, as can be observed in Figure (17).
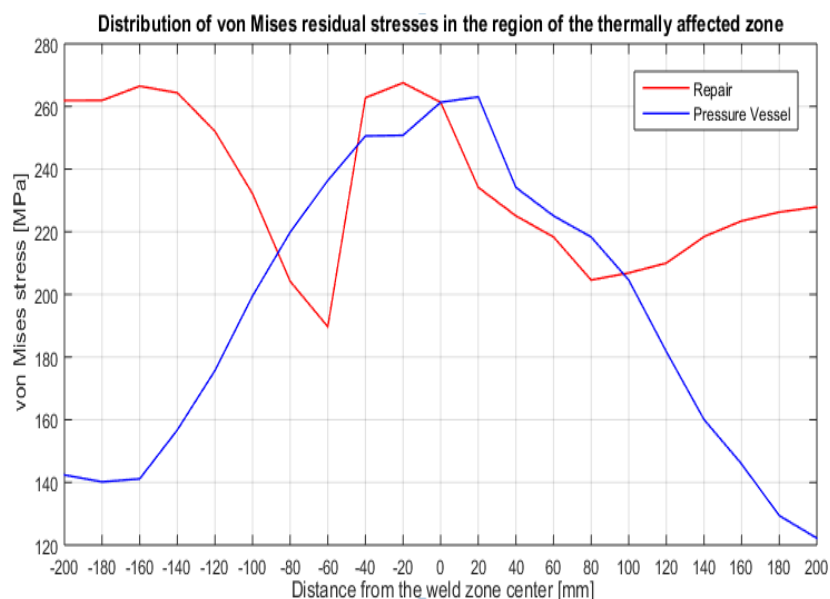

Figure 17 - Behavior of von Mises stresses in the pressure vessel and repair in the second longitudinal weld.

In Figure (17) the von Mises stress in the region of the thermally affected zone is observed, in the repair, the higher stresses are observed in the center of the weld, there being a relief of these stresses in the region between 25 and 55 mm in relation to the center of the weld, and after that interval these stresses increase again, reaching a value of between 230 and 260 MPa. For the von Mises stresses in the pressure vessel, the highest stresses are at the center of the weld, with a

value of about 260 MPa, and as it moves away from the center of the weld, these stresses decrease, reaching a value between 120 and 140 MPa.

4 CONCLUSION

The geometric modeling of the design and the data of the material must be correctly set, the design modeling strictly followed the ASME PCC-2-2015 standard to avoid problems in the simulation, and it is necessary to obtain all the correct properties of the material so that the results simulation are satisfactory and convergent. In general, it was observed that the greatest longitudinal, tangential and von Mises stresses are located in the repair, which means that the repair absorbs the residual stresses that would be in the pressure vessel.

The longitudinal, tangential and von Mises stress distribution was obtained at points near the weld, in the repair and in the pressure vessel which is important to observe the behavior after cooling in those regions, and it was seen that the higher stresses occur in the center of the weld and in the repair there are peaks of residual longitudinal and tangential stress due to the change of geometry of the weld for the repair, causing the stresses to increase in that region.

In view of this, it can be concluded that a well-designed numerical analysis can be the best option for structural analysis in general equipment, due to the objectivity and agility with which it can reach the results that are closer to reality. In addition, numerical analysis is of fundamental importance in the control and monitoring of the structural integrity of this equipment. The MEF has been gaining ground in these inspection works that can define the locations for the inspections.

5 REFERENCES

ALMEIDA, J.I.L. (2012). "Análise Numérica da Integridade Estrutural de Vasos de Pressão com Corrosão Usando a Norma API 579", Dissertação de Mestrado, João Pessoa.

BAN, H., SHI G., et al. (2013). "Residual Stress of 460 MPa High Strength Steel Welded I Section: Experimental Investigation and Modeling", International Journal of Steel Structures, 13(4), 691-705.

BORGES, M.F., BRAGA, S.S., et al. (2013). "Finite Element Analysis of Repair Technique on In-Service Pipeline with Dent". IBP 1325_13, Rio Pipeline Conference & Exposition;

HIRSCH, T.; MACHADO, R.; CAMPOS, M. F. (2006). "Tensões Residuais em Aços Avaliados por Difração de Raios-X: Diferença Entre Micro e Macro Tensões Residual", III Workshop sobre textura, São Paulo, p. 115-131;

LU, J.(2005). "Handbook of Measurements of Residual Stress", Vol. 2, Ed. SEM, 2ed;

MARTINEZ, L.L.(1997). "Fatigue behavior of welded high strengthsteels". Department of Aeronautics, KTH, Report No. 97-30;

RYBICKI, E.F., STONESIFER, R.B. (1979). "Computation of Residual Stresses Due to Multipass Welds in Piping Systems", ASME Trans J Pressure Vessel Technology Vol. 101, May, pp149-154;

COMO CITAR ESTE ARTIGO:

SOBRE OS AUTORES

J. I. L. ALMEIDA
Professor Adjunto da Escola Politécnica da Universidade Federal da Bahia. Doutorado em Engenharia Mecânica pela Universidade Federal da Paraíba na área de Petróleo e Gás Natural com ênfase em reparos e integridade estrutural em vasos de pressão pela Fitness for Service e análise de Elementos Finitos (2017). Mestrado em Engenharia Mecânica pela Universidade Federal da Paraíba na área de Dinâmica e Controle de Sistemas (2012), linha de pesquisa Metrologia Assistida por Computador voltado para a Integridade Estrutural em Vasos de Pressão. Graduado em Engenharia Mecânica pela Universidade Federal da Paraíba (2010). Tem experiência em ensaios não destrutivos, Fitness for Service (Adequação ao Serviço), integridade estrutural em vasos de pressão, corrosão e mecânica computacional. Atualmente integra o Grupo de Pesquisa em Integridade e Inspeção (GPII) do Laboratório de Integridade e Inspeção do Departamento de Engenharia Mecânica pela Universidade Federal da Paraíba. E-mail: jayann.ismar@gmail.com
ORCID ID: https://orcid.org/0000-0001-6899-920X

M. C. RODRIGUES
Professor do Departamento de Engenharia Mecânica da UFPB em João Pessoa onde é pesquisador de Grupos de Pesquisas de Integridade e Inspeção (GPII). Coordenador do Laboratório de Integridade e Inspeção (LabII). Possui Doutorado em Engenharia Mecânica pela Universidade Federal da Paraíba (2007) na área de Dinâmica e Controle de Sistemas e Integridade estrutural de poços de petróleo (Hastes de Bombeio BCP). Mestrado em Engenharia Mecânica pela Universidade Federal de Campina Grande (2003) onde foi bolsista da ANP/PRH-25 e graduação em Engenharia Mecânica pela Universidade Federal da Paraíba (2000). Tem experiência na área de engenharia mecânica (manutenção) e na área de petróleo (workover e completação de poços), atuando principalmente nos seguintes temas: integridade estrutural de equipamentos de poços de petróleo, elementos finitos, análise modal, trabalhos de simulação em plataforma semi-submersível, vibrações mecânicas e atualmente trabalha com Ensaios Não-Destrutivos (Ultra-som) e Vasos de Pressão (API 579 Fitness for service). E-mail: celo_cr@yahoo.com.br
ORCID ID: https://orcid.org/0000-0002-3663-5097

P. F. CAVALCANTE
Possui graduação em Engenharia Mecânica pela Universidade Federal da Paraíba (1993), mestrado em Engenharia Mecânica pela Universidade Estadual de Campinas (1997) e doutorado em Engenharia Mecânica pela Universidade Estadual de Campinas (2001). Atualmente é professora Associada I da Universidade Federal da Bahia. Tem experiência na área de Engenharia Mecânica, com ênfase em Dinâmica de Rotores, atuando principalmente nos seguintes temas: umbilicais, análise modal, elementos finitos, análise estrutural e desenvolvimento de produto. E-mail: pplegal2@yahoo.com
ORCID ID: https://orcid.org/0000-0003-2742-7445

14